Supporting Information: Detecting Chirality in Two-Terminal Electronic Nanodevices

Xu Yang,[1,*] Caspar H. van der Wal,[1] and Bart J. van Wees[1]

[1] *Zernike Institute for Advanced Materials, University of Groningen, NL-9747AG Groningen, The Netherlands*

CONTENTS

A. Comparison to Absolute Asymmetric (Chemical) Synthesis

Absolute asymmetric synthesis refers to chemical reactions starting from achiral or racemic reactants but yield chiral products with a net enantiomeric excess. Generally, it requires the presence of a truly chiral external influence, which, according to Barron [S1], is a physical quantity that can appear in two degenerate forms (e.g. opposite signs of one physical quantity, or parallel and anti-parallel alignments of two vectors), which are interconverted by space-inversion but not by time-reversal. Following this, the lone influence of a magnetic field, which reverses sign under time-reversal but not space-inversion, is not truly chiral, and therefore should not induce absolute asymmetric synthesis.

Just like Onsager reciprocity, this true-chirality consideration is based on microscopic reversibility, and therefore is strict only in the linear response regime (in the vicinity of thermodynamic equilibrium). Barron later pointed out that [S2], in a chemical reaction that would yield a racemic mixture (of enantiomers), the presence of a magnetic field allows different reaction rates toward opposite enantiomers. This creates an enantiomeric excess away from equilibrium, which should eventually disappear as the system returns to equilibrium. However, if the nonequilibrium enantiomeric excess is amplified, for example by self-assembly or crystallization, absolute asymmetric synthesis can be induced, and this was later demonstrated experimentally [S3, S4].

This shows that a time-reversal-breaking influence (the magnetic field), albeit not being truly chiral, can still distinguish and separate enantiomers away from thermodynamic equilibrium. By the same token, in the 2T circuit that we discuss, the FM breaks time reversal symmetry and can therefore indeed distinguish enantiomers away from equilibrium, i.e. in the nonlinear regime. Therefore, the nonlinear conductance of the 2T circuit may depend on the chirality of the circuit component, as well as the magnetization direction of the FM.

B. Beyond the Landauer Formula

The Landauer formula describes the electrical conductance of a conductor using its scattering properties [S5]. Particularly, it expresses conductance in terms of transmission probabilities between electrodes, but does not require the use of reflection probabilities. Moreover, it considers that the charge (and spin) transport are solely driven by charge biases, and neglects possible spin accumulations in the circuit [S6]. For a 2T device, it allows two independent parameters (charge and spin transmission probabilities) for the description of coupled charge and spin transport.

We point out here that a full description of the coupled charge and spin transport must extend beyond the conventional (spin-resolved) Landauer formula, and include also the (spin-flip) reflection terms and the buildup of spin accumulations, which also act as driving forces of the transport. This point was earlier raised for an FM–normal metal system [S7]. Following this, we need to characterize the (twofold rotationally symmetric) chiral component using four independent parameters, see the matrix in eq. S13, contrasting to the two parameters mentioned earlier.

Using this extended Landauer formula that is similar to a Büttiker multiterminal analysis, we can fully (in terms of charge and spin) account for how a generic spin–charge converter responds to charge and spin driving forces. This response can be described using the transport matrices that our main text focuses on. Note that although in this work we derive these transport matrices using the extended Landauer formula, it does not limit the general validity of the transport matrix formalism. The transport matrices can be alternatively derived using other methods, and can be extended to the nonlinear regime by including energy or bias dependences. The symmetry/asymmetry of the transport matrix in the linear/nonlinear response regime is fundamentally related to the (breaking of) Onsager reciprocity, and does not depend on how the transport matrix itself is derived.

C. Nonunitarity for Generating CISS and Energy Relaxation for Generating MR

The generation of CISS requires the presence of nonunitary effects inside the chiral component, because the Kramers degeneracy would otherwise require equal transmission probabilities for opposite spin orientations [S8, S9]. These nonunitary effects break the phase information of a transmitting electron, but does not necessarily alter its energy.

The presence of these nonunitary effects only allows the generation of CISS, but does not guarantee the generation of a 2T MR. These nonunitary effects do not (necessarily) break the Onsager reciprocity, and therefore a 2T MR is still forbidden in the linear response regime. Even when considering energy-dependent transport in the nonlinear regime, since at each energy level the Onsager reciprocity still holds, a 2T MR cannot arise.

The emergence of MR, as we discussed, requires energy relaxation in the device. These relaxation processes not only break the phase information, but also alter the energy of the electrons, and rearrange them according to Fermi–Dirac

distribution. We have assumed that they do not change the spin orientation of the electrons. In principle, we can also include spin relaxation in the node, which we expect to reduce the MR without changing its sign.

D. Spin and Charge Transport in a Nonmagnetic Chiral Component

In the main text we introduced the spin-space transmission and reflection matrices for the right-moving electrons in a (nonmagnetic) chiral component (eq. 1)

$$\mathbb{T}_{\triangleright} = \begin{pmatrix} t_{\rightarrow\rightarrow} & t_{\leftarrow\rightarrow} \\ t_{\rightarrow\leftarrow} & t_{\leftarrow\leftarrow} \end{pmatrix}, \quad \mathbb{R}_{\triangleright} = \begin{pmatrix} r_{\rightarrow\rightarrow} & r_{\leftarrow\rightarrow} \\ r_{\rightarrow\leftarrow} & r_{\leftarrow\leftarrow} \end{pmatrix}. \tag{S1}$$

For the left-moving electrons, the matrices are the time-reversed forms of the above

$$\mathbb{T}_{\triangleleft} = \begin{pmatrix} t_{\leftarrow\leftarrow} & t_{\rightarrow\leftarrow} \\ t_{\leftarrow\rightarrow} & t_{\rightarrow\rightarrow} \end{pmatrix}, \quad \mathbb{R}_{\triangleleft} = \begin{pmatrix} r_{\leftarrow\leftarrow} & r_{\rightarrow\leftarrow} \\ r_{\leftarrow\rightarrow} & r_{\rightarrow\rightarrow} \end{pmatrix}. \tag{S2}$$

Note that these matrices are not suitable for describing magnetic components where time-reversal symmetry is not preserved. Also, we have assumed the chiral component to be symmetric (i.e. a twofold rotational symmetry with axis perpendicular to the electron pathway, this ensures that for oppositely moving electrons, the spin polarization only changes sign).

We use spin-space column vector to describe electrochemical potentials and currents on both sides of the molecule, and following ref. S10 we have

$$\begin{pmatrix} I_{L\rightarrow} \\ I_{L\leftarrow} \end{pmatrix} = -\frac{Ne}{h}\left[(\mathbb{I} - \mathbb{R}_{\triangleright})\begin{pmatrix} \mu_{L\rightarrow} \\ \mu_{L\leftarrow} \end{pmatrix} - \mathbb{T}_{\triangleleft}\begin{pmatrix} \mu_{R\rightarrow} \\ \mu_{R\leftarrow} \end{pmatrix}\right], \tag{S3a}$$

$$-\begin{pmatrix} I_{R\rightarrow} \\ I_{R\leftarrow} \end{pmatrix} = -\frac{Ne}{h}\left[(\mathbb{I} - \mathbb{R}_{\triangleleft})\begin{pmatrix} \mu_{R\rightarrow} \\ \mu_{R\leftarrow} \end{pmatrix} - \mathbb{T}_{\triangleright}\begin{pmatrix} \mu_{L\rightarrow} \\ \mu_{L\leftarrow} \end{pmatrix}\right], \tag{S3b}$$

where N is the number of spin-degenerate channels.

We define charge electrochemical potential $\mu = (\mu_{\rightarrow} + \mu_{\leftarrow})/2$ and spin accumulation $\mu_s = (\mu_{\rightarrow} - \mu_{\leftarrow})/2$, as well as charge current $I = I_{\rightarrow} + I_{\leftarrow}$ and spin current $I_s = I_{\rightarrow} - I_{\leftarrow}$. We describe here both charge and spin in electrical units.

Following these definitions, we have

$$I = I_{L\rightarrow} + I_{L\leftarrow} = I_{R\rightarrow} + I_{R\leftarrow}, \tag{S4a}$$

$$I_{sL} = I_{L\rightarrow} - I_{L\leftarrow}, \tag{S4b}$$

$$I_{sR} = I_{R\rightarrow} - I_{R\leftarrow}, \tag{S4c}$$

$$\mu_L = (\mu_{L\rightarrow} + \mu_{L\leftarrow})/2, \tag{S4d}$$

$$\mu_R = (\mu_{R\rightarrow} + \mu_{R\leftarrow})/2, \tag{S4e}$$

$$\mu_{sL} = (\mu_{L\rightarrow} - \mu_{L\leftarrow})/2, \tag{S4f}$$

$$\mu_{sR} = (\mu_{R\rightarrow} - \mu_{R\leftarrow})/2. \tag{S4g}$$

Combining eq. S3 and S4, we derive

$$\begin{pmatrix} I \\ -I_{sL} \\ I_{sR} \end{pmatrix} = -\frac{Ne}{h}\begin{pmatrix} t & s & s \\ P_r r & \gamma_r & \gamma_t \\ P_t t & \gamma_t & \gamma_r \end{pmatrix}\begin{pmatrix} \mu_L - \mu_R \\ \mu_{sL} \\ \mu_{sR} \end{pmatrix}, \tag{S5}$$

which is eq. 2 in the main text, and $\mu_L - \mu_R = -eV$ is induced by a bias voltage V.

The matrix elements are

$$t = t_{\rightarrow\rightarrow} + t_{\rightarrow\leftarrow} + t_{\leftarrow\rightarrow} + t_{\leftarrow\leftarrow}, \tag{S6a}$$
$$r = r_{\rightarrow\rightarrow} + r_{\rightarrow\leftarrow} + r_{\leftarrow\rightarrow} + r_{\leftarrow\leftarrow} = 2 - t, \tag{S6b}$$
$$\gamma_t = t_{\rightarrow\rightarrow} - t_{\rightarrow\leftarrow} - t_{\leftarrow\rightarrow} + t_{\leftarrow\leftarrow}, \tag{S6c}$$
$$\gamma_r = r_{\rightarrow\rightarrow} - r_{\rightarrow\leftarrow} - r_{\leftarrow\rightarrow} + r_{\leftarrow\leftarrow} - 2, \tag{S6d}$$
$$P_t = (t_{\rightarrow\rightarrow} - t_{\rightarrow\leftarrow} + t_{\leftarrow\rightarrow} - t_{\leftarrow\leftarrow})/t, \tag{S6e}$$
$$P_r = (r_{\rightarrow\rightarrow} - r_{\rightarrow\leftarrow} + r_{\leftarrow\rightarrow} - r_{\leftarrow\leftarrow})/r, \tag{S6f}$$
$$s = t_{\rightarrow\rightarrow} + t_{\rightarrow\leftarrow} - t_{\leftarrow\rightarrow} - t_{\leftarrow\leftarrow} \tag{S6g}$$
$$= -r_{\rightarrow\rightarrow} - r_{\rightarrow\leftarrow} + r_{\leftarrow\rightarrow} + r_{\leftarrow\leftarrow}. \tag{S6h}$$

For $r = 2 - t$ and the two expressions of s, we have used the condition of charge conservation

$$t_{\rightarrow\rightarrow} + t_{\rightarrow\leftarrow} + r_{\rightarrow\rightarrow} + r_{\rightarrow\leftarrow} = 1, \tag{S7a}$$
$$t_{\leftarrow\rightarrow} + t_{\leftarrow\leftarrow} + r_{\leftarrow\rightarrow} + r_{\leftarrow\leftarrow} = 1. \tag{S7b}$$

Among the above matrix elements, P_t, P_r, and s change sign when the chirality is reversed. For achiral components where there is no spin selective transport, we have $P_t = P_r = s = 0$, and the transport matrix is symmetric.

Note that in eq. 2 we have defined the vector of currents (thermodynamic response) using $-I_{sL}$ and I_{sR}, so that the transport matrix is symmetric in the linear response regime. Following this, as shown in Figure 1, the chiral component acts as a source (or sink) of spin currents when biased.

We can rewrite γ_t and γ_r as transmission-dependent quantities

$$\gamma_r = r - (P_r r + s)/\eta_r - 2 = -t - (P_r r + s)/\eta_r, \tag{S8a}$$
$$\gamma_t = -t + (P_t t + s)/\eta_t, \tag{S8b}$$

where

$$\eta_r = \frac{r_{\leftarrow\rightarrow} - r_{\rightarrow\leftarrow}}{r_{\leftarrow\rightarrow} + r_{\rightarrow\leftarrow}}, \tag{S9a}$$
$$\eta_t = \frac{t_{\rightarrow\rightarrow} - t_{\leftarrow\leftarrow}}{t_{\rightarrow\rightarrow} + t_{\leftarrow\leftarrow}}, \tag{S9b}$$

are quantities between ± 1 and change sign under chirality reversal.

Next, for chiral components where P_t, P_r, and s are nonzero, the Onsager reciprocity requires the 3×3 matrix to be symmetric [S11], which gives

$$P_t t = P_r r = s, \tag{S10}$$

and therefore

$$t_{\rightarrow\leftarrow} = t_{\leftarrow\rightarrow}, \tag{S11a}$$
$$r_{\rightarrow\rightarrow} = r_{\leftarrow\leftarrow}, \tag{S11b}$$
$$t_{\rightarrow\rightarrow} - t_{\leftarrow\leftarrow} = r_{\leftarrow\rightarrow} - r_{\rightarrow\leftarrow}. \tag{S11c}$$

These expressions show that, for any finite P_t (spin polarization of transmitted electrons), P_r (spin polarization of reflected electrons) must also be nonzero and have the same sign, which then requires the presence of spin-flip reflections [S10]. This is again in agreement with the fundamental considerations based on zero charge and spin currents in electrodes at equilibrium.

Further, we obtain

$$\gamma_r = -(1 + 2P_t/\eta_r)t, \tag{S12a}$$
$$\gamma_t = -(1 - 2P_t/\eta_t)t. \tag{S12b}$$

which allows us to rewrite the transport matrix equation in terms of t

$$\begin{pmatrix} I \\ -I_{sL} \\ I_{sR} \end{pmatrix} = -\frac{Ne}{h} \begin{pmatrix} t & P_t t & P_t t \\ P_t t & -(1 + 2P_t/\eta_r)t & -(1 - 2P_t/\eta_t)t \\ P_t t & -(1 - 2P_t/\eta_t)t & -(1 + 2P_t/\eta_r)t \end{pmatrix} \begin{pmatrix} \mu_L - \mu_R \\ \mu_{sL} \\ \mu_{sR} \end{pmatrix}. \tag{S13}$$

Note that P_t, η_t, and η_r all change sign when the chirality is reversed, and t, P_t/η_t, and P_t/η_r are always positive.

In later discussions we connect the right-hand side of the nonmagnetic component to an electrode (see Figure 2a) where the spin accumulation μ_{sR} is zero and the spin current I_{sR} is irrelevant. This reduces the matrix equation to

$$\begin{pmatrix} I \\ -I_{sL} \end{pmatrix} = -\frac{Ne}{h} \begin{pmatrix} t & P_t t \\ P_t t & -(1+2P_t/\eta_r)t \end{pmatrix} \begin{pmatrix} \mu_L - \mu_R \\ \mu_{sL} \end{pmatrix}, \tag{S14}$$

which is equivalent to eq. 3 in the main text.

E. Spin and Charge Transport at an Achiral Ferromagnetic Tunnel Junction/Interface (FMTJ)

In an FM, time-reversal symmetry is broken and the Kramers degeneracy is lifted. The FMTJ provides a spin polarization to any current that flows through, and reciprocally, it generates a charge voltage upon a spin accumulation at its interface. In terms of spin and charge transport, the FMTJ effectively allows different conductances for electrons with opposite spins, and the difference depends on its spin polarization P_{FM}. Inside the FM, spin relaxation is strong and spin accumulation is negligible. For our discussions, the FM is always connected to the left-hand side of a node, we thus only consider the R interface of the FM with a spin accumulation μ_{sR} (in the node). Following the discussion provided in ref. S12, the spin-specific currents on the R-side are therefore

$$I_{\rightarrow} = -\frac{1}{e} G_{\rightarrow}[\mu_L - (\mu_R + \mu_{sR})], \tag{S15a}$$

$$I_{\leftarrow} = -\frac{1}{e} G_{\leftarrow}[\mu_L - (\mu_R - \mu_{sR})], \tag{S15b}$$

where $G_{\rightarrow(\leftarrow)}$ is the spin-specific tunnel conductance. We define the total conductance $G_{FM} = G_{\rightarrow} + G_{\leftarrow}$ and FM spin-polarization $P_{FM} = (G_{\rightarrow} - G_{\leftarrow})/(G_{\rightarrow} + G_{\leftarrow})$. We also introduce a transmission coefficient T ($0 \leqslant T \leqslant 2$) to distinguish G_{FM} from ideal transmission. The charge and spin currents on the R interface of the FM can thus be written as

$$\begin{pmatrix} I \\ I_{sR} \end{pmatrix} = -\frac{N'e}{h} \begin{pmatrix} T & -P_{FM}T \\ P_{FM}T & -T \end{pmatrix} \begin{pmatrix} \mu_L - \mu_R \\ \mu_{sR} \end{pmatrix}, \tag{S16}$$

where N' is the number of spin-degenerate channels in the FMTJ.

This matrix gives the spin and charge response of the FMTJ, and unlike for a chiral molecule, this matrix fulfills the Onsager reciprocity by being antisymmetric (opposite off-diagonal terms), because upon magnetic field and magnetization reversal, P_{FM} changes sign [S11].

F. Spin and Charge Transport in a Generic 2T Circuit

We consider a generic 2T circuit like the one shown in Figure 2a. Our goal here is to derive the quantities I, μ, and μ_s as a function of 2T bias $\mu_L - \mu_R$, by adapting eq. 3 and 4 in accordance with the notations in Figure 2a. We rewrite the transport matrices into conductance matrices, and obtain for the left and right side of the node

$$\begin{pmatrix} I \\ I_s \end{pmatrix} = -\frac{1}{e} \begin{pmatrix} G_1 & G_2 \\ G_3 & G_4 \end{pmatrix} \begin{pmatrix} \mu_L - \mu \\ \mu_s \end{pmatrix}, \tag{S17a}$$

$$\begin{pmatrix} I \\ -I_s \end{pmatrix} = -\frac{1}{e} \begin{pmatrix} g_1 & g_2 \\ g_3 & g_4 \end{pmatrix} \begin{pmatrix} \mu - \mu_R \\ \mu_s \end{pmatrix}. \tag{S17b}$$

At steady state the continuity condition requires the currents I and I_s are equal in both subequations. This condition allows us to derive

$$\begin{aligned} \mu &= \mu_R + \frac{G_3(G_2 - g_2) - G_1(G_4 + g_4)}{f} \ (\mu_L - \mu_R) \\ &= \mu_L - \frac{g_3(g_2 - G_2) - g_1(G_4 + g_4)}{f} \ (\mu_L - \mu_R), \end{aligned} \tag{S18a}$$

$$\mu_s = \frac{(G_3/G_1 + g_3/g_1)G_1 g_1}{f} \ (\mu_L - \mu_R), \tag{S18b}$$

$$I = \frac{G_1 g_2 g_3 + g_1 G_2 G_3 - G_1 g_1 (G_4 + g_4)}{f} \ (\mu_L - \mu_R), \tag{S18c}$$

where the coefficient f is

$$f = (G_3 - g_3)(G_2 - g_2) - (G_1 + g_1)(G_4 + g_4). \tag{S19}$$

Notably, f depends on $(G_3 - g_3)(G_2 - g_2)$, and for our linear-regime example using an FM with $G_2 = -G_3$ and a chiral component with $g_2 = g_3$, f only depends on $g_3^2 - G_3^2$, which remains unchanged when either the FM magnetization or the chirality is reversed. Moreover, the charge current I only depends on g_3^2 and G_3^2, and therefore also remains unchanged under magnetization or chirality reversal. In contrast, the spin accumulation μ_s depends on G_3 and g_3, and the charge distribution indicated by μ depends on $G_3 g_2$ or $g_3 G_2$. Both μ_s and μ therefore indeed change upon magnetization or chirality reversal, and can be detected using three-terminal or four-terminal measurements.

If the two circuit components would both be FM (antisymmetric G and g matrices) or both be chiral (symmetric G and g matrices), then the coefficient f contains the cross products $G_3 g_2$ and $G_2 g_3$, and therefore gives rise to a 2T current that does change upon magnetization or chirality reversal.

G. Reciprocity Breaking by Energy-Dependent Tunneling

Here we derive the energy dependence of the charge and spin tunneling through the FMTJ following the discussion by Jansen *et al.* [S12], and derive the subsequent nonlinear coupled charge and spin transport equations.

We consider a biased symmetric rectangular tunnel barrier with height Φ and width w between the FM and the node, as shown in Figure S1. The reference energy $\epsilon = 0$ is chosen as the average of μ_L and μ, so that the average barrier height does not change with bias. The bias voltage $V = -\Delta\mu/e$ is applied, so that $\mu_L = \Delta\mu/2$, $\mu = -\Delta\mu/2$, $\mu_\rightarrow = -\Delta\mu/2 + \mu_s$, and $\mu_\leftarrow = -\Delta\mu/2 - \mu_s$. For simplicity, we assume the barrier height (evaluated at the center of the tunnel barrier) is constant, the tunneling is one dimensional, and the electrostatic potential drop across the tunnel barrier is exactly $-eV$.

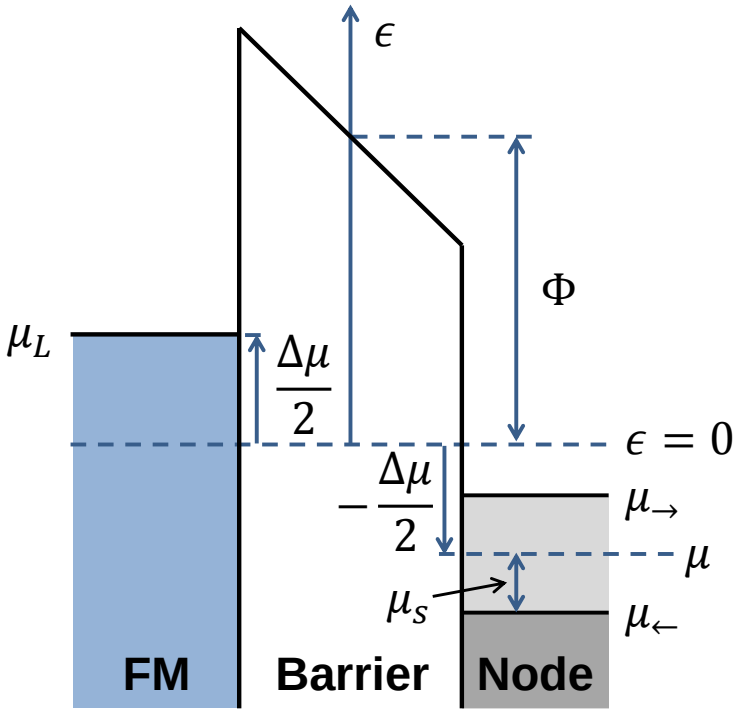

Figure S1. Energy diagram of the tunnel barrier at the ferromagnet interface. Details see text.

The energy-dependent electron tunnel transmission function is

$$T(\epsilon) = 2\exp\left(-\beta\ (\Phi - \epsilon)^{1/2}\right), \tag{S20}$$

where $\beta = 2w\sqrt{2m/\hbar^2}$, with m being the (effective) electron mass and $\hbar$ the reduced Planck's constant.

The total transmitted current is an energy-integral of two energy-dependent functions: (1). the transmission function $T(\epsilon)$, and (2) the voltage-dependent Fermi–Dirac distribution functions in both electrodes. The two parts dominate at different bias regimes with respect to the thermal activation energy k_BT, where k_B is the Boltzmann constant and T is temperature. For tunneling, typically we have $|eV| \gg k_BT$, and therefore we assume zero temperature for convenience. The Fermi–Dirac distribution function then becomes a Heaviside step function with the step at μ_L for the left electrode and at $\mu_\rightarrow$ and $\mu_\leftarrow$ for the two spin species in the node.

Assuming P_{FM} does not depend on energy, the energy-integrated tunnel current for each spin species through the FMTJ is

$$I_\rightarrow(\Delta\mu, \mu_s) = -\frac{N'e}{h}\ \frac{1+P_{FM}}{2}\ \int_{\mu_\rightarrow}^{\mu_L} T(\epsilon)\ d\epsilon, \tag{S21a}$$

$$I_\leftarrow(\Delta\mu, \mu_s) = -\frac{N'e}{h}\ \frac{1-P_{FM}}{2}\ \int_{\mu_\leftarrow}^{\mu_L} T(\epsilon)\ d\epsilon. \tag{S21b}$$

The range of the integrals can be rewritten as

$$\text{for } I_\rightarrow: \quad \int_{\mu_\rightarrow}^{\mu_L} d\epsilon = \int_{\mu}^{\mu_L} d\epsilon - \int_{\mu}^{\mu_\rightarrow} d\epsilon, \tag{S22a}$$

$$\text{for } I_\leftarrow: \quad \int_{\mu_\leftarrow}^{\mu_L} d\epsilon = \int_{\mu}^{\mu_L} d\epsilon + \int_{\mu_\leftarrow}^{\mu} d\epsilon. \tag{S22b}$$

We denote the two integrals on the right-hand side of the expressions $I^{(1)}_{\rightarrow(\leftarrow)}$ and $I^{(2)}_{\rightarrow(\leftarrow)}$ respectively, so that we have $I_\rightarrow = I^{(1)}_\rightarrow + I^{(2)}_\rightarrow$ and $I_\leftarrow = I^{(1)}_\leftarrow + I^{(2)}_\leftarrow$. The first integral $I^{(1)}_{\rightarrow(\leftarrow)}$ depends on the electrochemical potential difference across the barrier, $\Delta\mu$, and thus describes the bias-induced transport. In contrast, the second integral $I^{(2)}_{\rightarrow(\leftarrow)}$ depends on μ and μ_s in the node, and it vanishes when $\mu_s = 0$, and therefore it describes the spin-accumulation-induced correction to the first integral. We will treat the two integrals separately.

The bias-induced charge and spin currents are

$$\begin{aligned} I^{(1)} &= I^{(1)}_\rightarrow + I^{(1)}_\leftarrow \\ &= -\frac{N'e}{h}\int_{\mu}^{\mu_L} T(\epsilon)\ d\epsilon \\ &= -\frac{N'e}{h}\ \left(\overline{T}|^{\mu_L}_{\mu}\right)\ \Delta\mu, \end{aligned} \tag{S23a}$$

$$\begin{aligned} I^{(1)}_s &= I^{(1)}_\rightarrow - I^{(1)}_\leftarrow \\ &= -\frac{N'e}{h}\ P_{FM}\ \int_{\mu}^{\mu_L} T(\epsilon)\ d\epsilon \\ &= -\frac{N'e}{h}\ \left(P_{FM}\ \overline{T}|^{\mu_L}_{\mu}\right)\ \Delta\mu, \end{aligned} \tag{S23b}$$

where the averaged transmission within the bias window is defined as

$$\overline{T}|^{\mu_L}_{\mu} = \frac{1}{\Delta\mu}\ \int_{\mu}^{\mu_L}\ T(\epsilon)\ d\epsilon. \tag{S24}$$

Note that when $\Delta\mu$ changes sign, the integral changes sign too, and therefore $\overline{T}|^{\mu_L}_{\mu}$ is an even function of $\Delta\mu$.

For the spin-accumulation-induced currents, we have

$$\begin{aligned} &I^{(2)} = I^{(2)}_\rightarrow + I^{(2)}_\leftarrow \\ &= -\frac{N'e}{h}\left[-\frac{1+P_{FM}}{2}\int_{\mu}^{\mu_\rightarrow} T(\epsilon)d\epsilon + \frac{1-P_{FM}}{2}\int_{\mu_\leftarrow}^{\mu} T(\epsilon)d\epsilon\right] \\ &\approx -\frac{N'e}{h}\left(-P_{FM}T|_{\epsilon=\mu}\right)\cdot\mu_s, \end{aligned} \tag{S25a}$$

$$
\begin{aligned}
I_s^{(2)} &= I_{\rightarrow}^{(2)} - I_{\leftarrow}^{(2)} \\
&= -\frac{N'e}{h}\left[-\frac{1+P_{FM}}{2}\int_{\mu}^{\mu_{\rightarrow}} T(\epsilon)d\epsilon - \frac{1-P_{FM}}{2}\int_{\mu_{\leftarrow}}^{\mu} T(\epsilon)d\epsilon\right] \\
&\approx -\frac{N'e}{h}\left(-T|_{\epsilon=\mu}\right)\cdot\mu_s,
\end{aligned}
\tag{S25b}
$$

where the approximation is taken under the assumption that $\mu_s \ll \Delta\mu$, so that $T(\epsilon)$ is approximately a constant within the energy range from $\mu_{\leftarrow}$ to $\mu_{\rightarrow}$, and thus they are evaluated at $\epsilon = \mu = -\Delta\mu/2$. The energy dependence of $I^{(2)}$ and $I_s^{(2)}$ follows that of $T(\epsilon)$ (eq. S20).

We can now rewrite eq. S23 and S25 into matrix form

$$
\begin{pmatrix} I \\ I_s \end{pmatrix} = -\frac{N'e}{h}\begin{pmatrix} \overline{T}|_{\mu}^{\mu_L} & -P_{FM}T|_{\epsilon=\mu} \\ P_{FM}\overline{T}|_{\mu}^{\mu_L} & -T|_{\epsilon=\mu} \end{pmatrix}\begin{pmatrix} \mu_L - \mu \\ \mu_s \end{pmatrix},
\tag{S26}
$$

which is eq. 6 in the main text. The different off-diagonal terms demonstrate the breaking of Onsager reciprocity in the nonlinear regime, since one of them depends on the integral of the transmission function, while the other depends on the transmission function itself. In the linear response regime ($\mu_L \approx \mu$), the two terms differ only by sign.

We rewrite the above into

$$
\begin{pmatrix} I \\ I_s \end{pmatrix} = -\frac{1}{e}\begin{pmatrix} G_1 & G_2 \\ G_3 & G_4 \end{pmatrix}\begin{pmatrix} \mu_L - \mu \\ \mu_s \end{pmatrix},
\tag{S27}
$$

so that the matrix elements represent conductance, where $G_2 = (N'e^2/h)\cdot(-P_{FM}T|_{\epsilon=\mu})$ and $G_3 = (N'e^2/h)\cdot(P_{FM}\overline{T}|_{\mu}^{\mu_L})$. In Figure S2, we plot G_2 and G_3 as a function of bias across the FMTJ $[(\mu_L - \mu)/e]$ for $P_{FM} = -0.5$ and $N' = 1000$, values that are used to calculate the I–V curves in Figure 2d (for other parameters see later in SI.I).

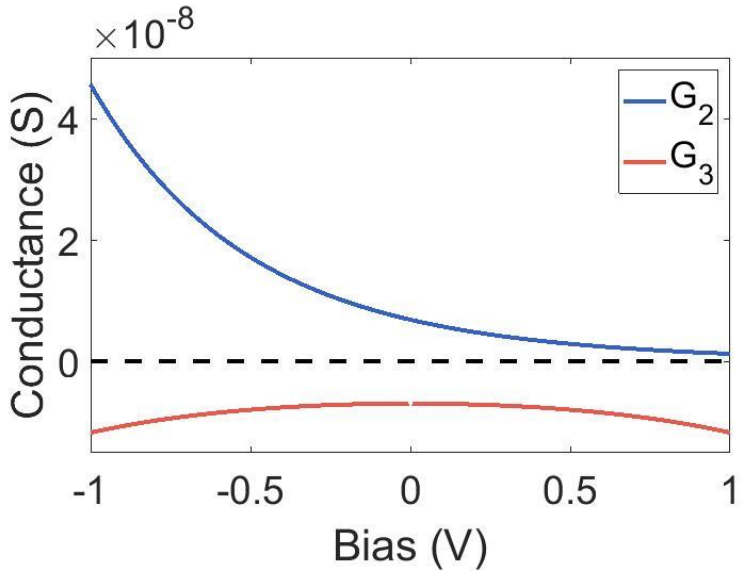

Figure S2. Bias dependence of the off-diagonal elements of the conductance matrix describing tunneling through the FMTJ.

Note that $G_2 = -G_3$ at zero bias, as required by Onsager reciprocity in the linear response regime. The breaking of reciprocity in the nonlinear regime is exhibited by the unequal absolute values of G_2 and G_3 away from zero bias. Here G_2 is increases monotonically with decreasing bias, while G_3 is symmetric in bias and obtains minimum (absolute value) at zero bias.

H. Reciprocity Breaking by Thermally Activated Resonant Transmission Through Molecular Orbitals

We discuss here the effect of the Fermi–Dirac distribution of electrons using resonant transmission through discrete molecular orbitals (MOs), specifically the lowest-unoccupied molecular orbital (LUMO) and the highest-occupied

molecular orbital (HOMO). This is illustrated in Figure S3. We assume here the LUMO and HOMO levels are fixed at energies ϵ_{LU} and $-\epsilon_{HO}$ respectively ($\epsilon_{LU}, \epsilon_{HO} > 0$), with $\epsilon = 0$ defined as the average of the two (charge) electrochemical potentials on both sides of the molecule. The nonlinearity is now assumed to be fully due to the Fermi–Dirac distribution $F(\epsilon, \mu)$, which is different for the node and the electrode, and is also different for the two spin species in the node when a spin accumulation is considered.

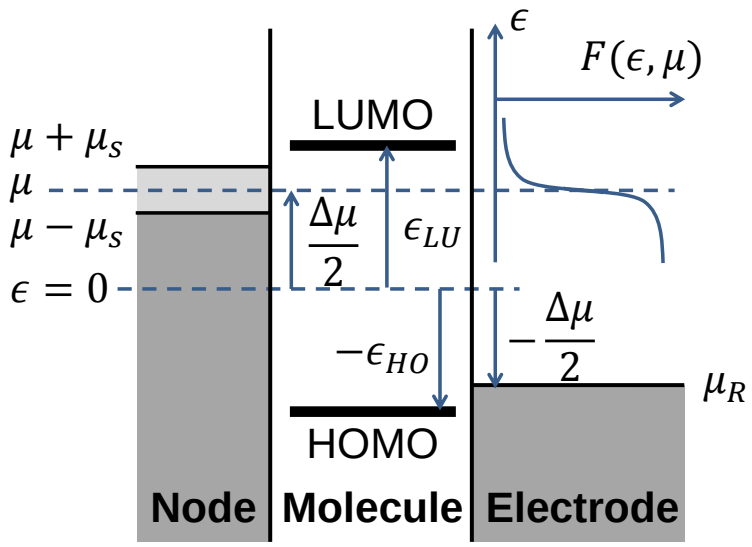

Figure S3. Energy diagram of the electron transmission through molecular orbitals.

Consider the geometry in Figure S3, at a given bias $\Delta\mu$ and a spin accumulation μ_s in the node, the spin-specific Fermi–Dirac functions for the two spin species in the node are

$$F_{L\rightarrow}(\epsilon, \Delta\mu, \mu_s) = \frac{1}{\exp\left(\frac{\epsilon - \Delta\mu/2 - \mu_s}{k_B T}\right) + 1}, \tag{S28a}$$

$$F_{L\leftarrow}(\epsilon, \Delta\mu, \mu_s) = \frac{1}{\exp\left(\frac{\epsilon - \Delta\mu/2 + \mu_s}{k_B T}\right) + 1}, \tag{S28b}$$

where we used subscript L to denote the node because its located on the left side of the molecule.

The Fermi–Dirac function in the node (neglecting the spin accumulation) and in the right electrode are

$$F_L(\epsilon, \Delta\mu) = \frac{1}{\exp\left(\frac{\epsilon - \Delta\mu/2}{k_B T}\right) + 1}, \tag{S29a}$$

$$F_R(\epsilon, \Delta\mu) = \frac{1}{\exp\left(\frac{\epsilon + \Delta\mu/2}{k_B T}\right) + 1}. \tag{S29b}$$

We model the resonant transmission through the MOs as energy-dependent transmission probability $t(\epsilon)$ that is only nonzero at the LUMO and the HOMO levels, which it is described by

$$t(\epsilon) = t_{LU}\delta(\epsilon - \epsilon_{LU}) + t_{HO}\delta(\epsilon + \epsilon_{HO}), \tag{S30}$$

where t_{LU} and t_{HO} are the transmission probabilities through the LUMO and the HOMO, respectively, and $\delta(\epsilon)$ is a Dirac delta function.

An exact calculation should separately address the two spin orientations separately, but for our assumption of $\mu_s \ll \Delta\mu$, we will directly start from the linear-regime equation of coupled charge and spin transport (eq. S14)

$$\begin{pmatrix} I \\ -I_{sL} \end{pmatrix} = -\frac{Ne}{h} \begin{pmatrix} t & P_t t \\ P_t t & -(1 + 2P_t/\eta_r)t \end{pmatrix} \begin{pmatrix} \mu - \mu_R \\ \mu_s \end{pmatrix}. \tag{S31}$$

This gives the charge current I

$$I = -\frac{Ne}{h}\left[t(\mu_L - \mu_R) + P_t t(\mu_{L\rightarrow} - \mu_{L\leftarrow})/2\right], \tag{S32}$$

where we used $\mu_{L\rightarrow} = \mu + \mu_s$ and $\mu_{L\leftarrow} = \mu - \mu_s$.

At finite temperature, the two terms in the square bracket on the right-hand side of the equation should each be replaced by an energy-integral of the electron transmission function modified by the voltage- and temperature-dependent Fermi–Dirac distributions in both electrodes. We denote the two terms $I^{(1)}$ and $I^{(2)}$, and the first term is

$$\begin{aligned} I^{(1)} &= \int_{-\infty}^{\infty} t(\epsilon)\left[F_L(\epsilon,\Delta\mu) - F_R(\epsilon,\Delta\mu)\right] d\epsilon \\ &= t_{LU}\left[F_L(\epsilon_{LU},\Delta\mu) - F_R(\epsilon_{LU},\Delta\mu)\right] \\ &\quad + t_{HO}\left[F_L(-\epsilon_{HO},\Delta\mu) - F_R(-\epsilon_{HO},\Delta\mu)\right]. \end{aligned} \tag{S33}$$

We denote

$$\mathcal{F}_\epsilon(\Delta\mu) = \frac{1}{\Delta\mu}\left[F_L(\epsilon,\Delta\mu) - F_R(\epsilon,\Delta\mu)\right], \tag{S34}$$

to highlight the transmission at energy ϵ and under bias $\Delta\mu$. In this manner, we can write

$$I^{(1)} = \left[t_{LU}\ \mathcal{F}_{\epsilon_{LU}}(\Delta\mu) + t_{HO}\ \mathcal{F}_{-\epsilon_{HO}}(\Delta\mu)\right]\ \Delta\mu. \tag{S35}$$

Similarly, at finite temperature, the second term $I^{(2)}$ becomes

$$\begin{aligned} & I^{(2)} \\ =& \frac{P_t}{2}\left(t_{LU}\left[F_{L\rightarrow}(\epsilon_{LU},\Delta\mu,\mu_s) - F_{L\leftarrow}(\epsilon_{LU},\Delta\mu,\mu_s)\right]\right. \\ &\left. + t_{HO}\left[F_{L\rightarrow}(-\epsilon_{HO},\Delta\mu,\mu_s) - F_{L\leftarrow}(-\epsilon_{HO},\Delta\mu,\mu_s)\right]\right). \end{aligned} \tag{S36}$$

We define

$$\begin{aligned} & \mathcal{F}'_{L,\epsilon}(\Delta\mu) \\ =& \frac{1}{2\mu_s}\ \left[F_{L\rightarrow}(\epsilon,\Delta\mu,\mu_s) - F_{L\leftarrow}(\epsilon,\Delta\mu,\mu_s)\right] \\ \approx& \frac{\partial[F_L(\epsilon,\Delta\mu)]}{\partial\Delta\mu}, \end{aligned} \tag{S37}$$

where the approximation is taken under the assumption of $\mu_s \ll \Delta\mu$.

With this, we have

$$I^{(2)} = P_t\left[t_{LU}\ \mathcal{F}'_{L,\epsilon_{LU}}(\Delta\mu) + t_{HO}\ \mathcal{F}'_{L,-\epsilon_{HO}}(\Delta\mu)\right]\mu_s. \tag{S38}$$

Similarly, the expression of $-I_{sL}$ at finite temperature can also be derived from the linear regime expression. The nonlinear coupled spin and charge transport equation, due to the thermally activated resonant transmission via the LUMO and the HOMO levels, is therefore

$$\begin{pmatrix} I \\ -I_{sL} \end{pmatrix} = -\frac{Ne}{h}\begin{pmatrix} t_{LU}\ \mathcal{F}_{\epsilon_{LU}}(\Delta\mu) + t_{HO}\ \mathcal{F}_{-\epsilon_{HO}}(\Delta\mu) & P_t[t_{LU}\ \mathcal{F}'_{L,\epsilon_{LU}}(\Delta\mu) + t_{HO}\ \mathcal{F}'_{L,-\epsilon_{HO}}(\Delta\mu)] \\ P_t[t_{LU}\ \mathcal{F}_{\epsilon_{LU}}(\Delta\mu) + t_{HO}\ \mathcal{F}_{-\epsilon_{HO}}(\Delta\mu)] & -(1+2P_t/\eta_r)\ [t_{LU}\ \mathcal{F}'_{L,\epsilon_{LU}}(\Delta\mu) + t_{HO}\ \mathcal{F}'_{L,-\epsilon_{HO}}(\Delta\mu)] \end{pmatrix}\begin{pmatrix} \mu - \mu_R \\ \mu_s \end{pmatrix}, \tag{S39}$$

where we have assumed P_t, η_r do not depend on energy.

The breaking of reciprocity arises from the different forms of the off-diagonal terms of the transport matrix. While the bottom-left term scales with the electron occupation function, the top-right terms scales with its derivative. In the linear response regime, the two terms are equal and the matrix is symmetric.

If required, this nonlinear transport equation can be easily extended to the 3×3 matrix for a generalized situation considering also a spin accumulation μ_{sR} on the right-hand side of the molecule. Then the third column will be modified in a similar way as the second column, but instead using the derivative of the electron occupation function in the right electrode $F_R(\epsilon,\Delta\mu)$.

Similar to the case of FMTJ, we can rewrite the above equation into

$$\begin{pmatrix} I \\ -I_s \end{pmatrix} = -\frac{1}{e}\begin{pmatrix} g_1 & g_2 \\ g_3 & g_4 \end{pmatrix}\begin{pmatrix} \mu - \mu_R \\ \mu_s \end{pmatrix}, \tag{S40}$$

where the matrix elements represent conductances. We plot the off-diagonal terms as a function of bias across the molecule $[(\mu - \mu_R)/e]$ for transmission through the LUMO level ($t_{LU} = 1$, $t_{HO} = 0$, $\epsilon_{LU} = 0.6$ eV) for $P_t = 0.85$ and $N = 1000$, as shown in Figure S4.

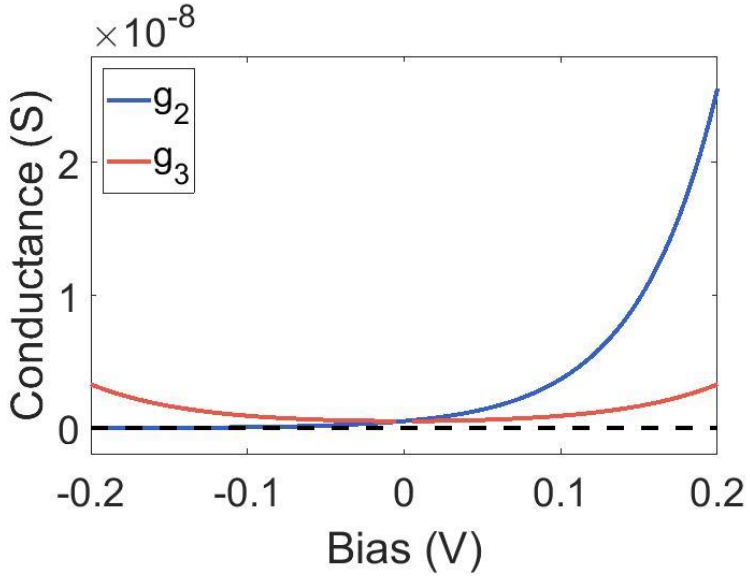

Figure S4. Bias dependence of the off-diagonal elements of the conductance matrix describing thermally activated conduction through the LUMO.

Note that $g_2 = g_3$ at zero bias, as required by Onsager reciprocity in the linear response regime. The reciprocity is broken as bias shifts away from zero, and the two conductances are no longer equal. Here g_2 increases monotonically with bias, while g_3 is bias-symmetric and reaches minimum at zero bias.

I. Parameters for Example I–V Curves

(1) For calculating the I–V curves in Figure 2d we have used the following parameters: Energy dependent FM tunnel transmission $T(\epsilon)$ for a tunnel barrier with height $\Phi = 2.1$ eV, and width $w = 1.0$ nm. The number of channels are set as $N' = 1000$ and $N = 5000$, the values are chosen taking into account the device length scale. For example, if using Ni as FM, when assuming each atom provides one channel, $N' = 1000$ corresponds to roughly an area of 100 nm^2. The transmission through the chiral component is set linear and uses the same transmission value as the FM tunnel barrier at zero bias. The polarization values are $P_{FM} = \pm 0.5$, $P_t = 0.85$, and the quantity η_r is set as $\eta_r = 0.9$. The same parameters are used to obtain the conductances in Figure S2.

(2) For calculating the I–V curves in Figure 3b and 3c we have used the following parameters: Temperature at 300 K, the LUMO level at $\epsilon_{LU} = 0.6$ eV, and the HOMO level at $-\epsilon_{HO} = -0.6$ eV. For Figure 3b, the LUMO transmission $t_{LU} = 1$ and the HOMO transmission $t_{HO} = 0$, while for Figure 3c the two values are interchanged. The number of channels are set as $N' = 1000$ and $N = 200$. The transmission through the FM tunnel barrier is set linear and uses the same transmission value as the FM tunnel barrier in case (1) at zero bias. The polarization values are $P_{FM} = \pm 0.5$, $P_t = 0.85$, and the quantity η_r is set as $\eta_r = 0.9$. The same parameters are used to obtain the conductances in Figure S4.

(3) For the chiral spin valve in Figure 4f, we use the same tunnel transmission function and the same barrier parameters as in case (1) for both chiral components (both nonlinear), and do not consider the thermally activated molecular level transmission. The number of channels are set as $N' = 1000$ and $N = 20000$. The first chiral component has polarization ± 0.5, and the second one 0.85, both have $\eta_r = 0.9$.

(d) For the example in Figure 4g, the tunnel barrier uses the same parameters as the FMTJ in case (1), but has zero spin polarization. The chiral component transmission is set linear and uses the same set of parameters as in case (1). The dashed curve is obtained by forcing $\mu_s = 0$ for all bias values.

J. Sign of the Nonlinear 2T MR

We summarize here, separately for the two nonlinear mechanisms, how the sign of the MR depends on chirality, charge carrier type, and bias direction. First of all, we define the MR for the device in Figure 2a following

$$MR = \frac{I_+ - I_-}{I_+ + I_-} \times 100\%, \tag{S41}$$

where I_+ represents the charge current measured with the FM polarization $P_{FM} > 0$, which corresponds to a spin-right polarization of the injected electrons, and I_- corresponds to the current measured when the FM generates a spin-left polarization.

For the bias direction, we describe it in terms of electron movement direction (opposite to charge current) with respect to the circuit components. For example, in Figure 2a, the positive bias voltage corresponds to an electron movement from the chiral component (CC) to the FMTJ.

For the (sign of) chirality, we label it as D and L. Here we (arbitrarily) assume that a D-chiral component favors the transmission of electrons with spins parallel to the electron momentum, while an L-chiral component favors the anti-parallel. The exact correspondence between the chirality and the favored spin orientation depends on the microscopic details of the spin orbit interaction.

According to these definitions, the sign of the MR is summarized in the following tables.

TABLE SI. Summary of the sign of MR for nonlinear tunneling through FMTJ

chirality	electron direction	carrier type	MR
D	CC to FMTJ	electron	+
L	CC to FMTJ	electron	-
D	FMTJ to CC	electron	-
L	FMTJ to CC	electron	+

TABLE SII. Summary of the sign of MR for nonlinear transmission through molecular orbitals

chirality	electron direction	carrier type	MR
D	CC to FMTJ	electron	+
L	CC to FMTJ	electron	-
D	FMTJ to CC	electron	-
L	FMTJ to CC	electron	+
D	CC to FMTJ	hole	-
L	CC to FMTJ	hole	+
D	FMTJ to CC	hole	+
L	FMTJ to CC	hole	-

K. Beyond Noninteracting-Electron Picture

We analyzed two elementary sources of energy dependence to illustrate the onset of MR in nonlinear regime: (a) energy-dependent tunnelling through the FMTJ (Figure 2), and (b) energy-dependent Fermi–Dirac distribution for resonant transmission through MOs(Figure 3). For convenience, both examples concentrated the role of electron–electron or electron–phonon interactions in the node for inducing energy relaxation, and considered a noninteracting-electron picture for transport through each individual circuit component. In practice, however, electron transport through

chiral molecules could also involve other many-body effects such as Coulomb blockade, Kondo effects, molecular deformation, and transport-induced chemical reactions [S13, S14].

We emphasize here, in three aspects, that our qualitative conclusions are not restricted by the noninteracting-electron picture that we use. Moreover, our quantitative results can in principle be improved by including the many-body effects when deriving the transport matrices.

First, the transport matrix formalism we introduced is generally valid. It describes the coupled charge and spin transport in generic spintronic nanodevices, which is (thermodynamically) driven by charge and spin chemical potentials. The symmetry/asymmetry of the transport matrices in the linear/nonlinear response regime is fundamentally related to the (breaking of) Onsager reciprocity. It does not depend on specific microscopic mechanisms. Based on this, we derived our main conclusion that MR signals can only arise in the nonlinear regime, and it requires energy-dependent transport and energy relaxation. This conclusion is therefore also fundamental and does not depend on detailed transport mechanisms.

Second, we identified how key factors such as bias direction, electron/hole transport, and chirality, codetermine the sign of the MR. These factors are also related to fundamental symmetry and the nature of electron transport, and do not depend on microscopic mechanisms.

Third, considering our two examples, the first one is also unaffected by electron–electron or electron–phonon interactions in the chiral component because it operates in the linear response regime. In the second example where we consider energy-dependent transport through the chiral component, potential many-body effects may indeed change the energy and bias dependence of the nonlinear transport, and thereby quantitatively affect the MR in the nonlinear regime.

We point out here that our formalism can be extended to include the role of many-body effects or other nonlinear mechanisms by deriving the transport matrices accordingly [S15, S16]. We encourage future studies to address these mechanisms to help identify their signatures in experimental results of the electrical detection of CISS.

* xu.yang@rug.nl

[S1] Barron, L. D. True and false chirality and absolute asymmetric synthesis. *Journal of the American Chemical Society* **108**, 5539–5542 (1986).

[S2] Barron, L. D. Reactions of chiral molecules in the presence of a time-non-invariant enantiomorphous influence: a new kinetic principle based on the breakdown of microscopic reversibility. *Chemical Physics Letters* **135**, 1–8 (1987).

[S3] Micali, N. *et al.* Selection of supramolecular chirality by application of rotational and magnetic forces. *Nature Chemistry* **4**, 201–207 (2012).

[S4] Banerjee-Ghosh, K. *et al.* Separation of enantiomers by their enantiospecific interaction with achiral magnetic substrates. *Science* **360**, 1331–1334 (2018).

[S5] Landauer, R. Conductance determined by transmission: probes and quantised constriction resistance. *Journal of Physics: Condensed Matter* **1**, 8099 (1989).

[S6] Büttiker, M., Imry, Y., Landauer, R. & Pinhas, S. Generalized many-channel conductance formula with application to small rings. *Physical Review B* **31**, 6207 (1985).

[S7] Brataas, A., Nazarov, Y. V. & Bauer, G. E. W. Finite-element theory of transport in ferromagnet–normal metal systems. *Physical Review Letters* **84**, 2481 (2000).

[S8] Bardarson, J. H. A proof of the Kramers degeneracy of transmission eigenvalues from antisymmetry of the scattering matrix. *Journal of Physics A: Mathematical and Theoretical* **41**, 405203 (2008).

[S9] Matityahu, S., Utsumi, Y., Aharony, A., Entin-Wohlman, O. & Balseiro, C. A. Spin-dependent transport through a chiral molecule in the presence of spin-orbit interaction and nonunitary effects. *Physical Review B* **93**, 075407 (2016).

[S10] Yang, X., van der Wal, C. H. & van Wees, B. J. Spin-dependent electron transmission model for chiral molecules in mesoscopic devices. *Physical Review B* **99**, 024418 (2019).

[S11] Onsager, L. Reciprocal relations in irreversible processes. II. *Physical Review* **38**, 2265 (1931).

[S12] Jansen, R. *et al.* Nonlinear electrical spin conversion in a biased ferromagnetic tunnel contact. *Physical Review Applied* **10**, 064050 (2018).

[S13] Díaz, E., Contreras, A., Hernández, J. & Domínguez-Adame, F. Effective nonlinear model for electron transport in deformable helical molecules. *Physical Review E* **98**, 052221 (2018).

[S14] Fransson, J. Chirality-induced spin selectivity: The role of electron correlations. *The Journal of Physical Chemistry Letters* **10**, 7126–7132 (2019).

[S15] Brandbyge, M., Mozos, J.-L., Ordejón, P., Taylor, J. & Stokbro, K. Density-functional method for nonequilibrium electron transport. *Physical Review B* **65**, 165401 (2002).

[S16] Meir, Y. & Wingreen, N. S. Landauer formula for the current through an interacting electron region. *Physical Review Letters* **68**, 2512 (1992).